

Article

Not peer-reviewed version

Bioactivity, Efficacy, and Safety of a Wound Healing Ointment with Medicinal Plant Bioactives: In Vitro and In Vivo Preclinical Evaluations

Juliana Floriano , [Daniel Rodrigues](#) , Rie Ohara , Nara Almeida , [Vanessa Soares](#) , [Patricia Sartorelli](#) ,
[Carlos Graeff](#) , [Simone Grecco](#) , Alejandra González , [Paulo D'Alpino](#) *

Posted Date: 10 October 2024

doi: 10.20944/preprints202410.0824.v1

Keywords: chronic wounds; wound care; natural compounds; biocompatibility; pre-clinical tests



Preprints.org is a free multidiscipline platform providing preprint service that is dedicated to making early versions of research outputs permanently available and citable. Preprints posted at Preprints.org appear in Web of Science, Crossref, Google Scholar, Scilit, Europe PMC.

Copyright: This is an open access article distributed under the Creative Commons Attribution License which permits unrestricted use, distribution, and reproduction in any medium, provided the original work is properly cited.

Disclaimer/Publisher's Note: The statements, opinions, and data contained in all publications are solely those of the individual author(s) and contributor(s) and not of MDPI and/or the editor(s). MDPI and/or the editor(s) disclaim responsibility for any injury to people or property resulting from any ideas, methods, instructions, or products referred to in the content.

Article

Bioactivity, Efficacy, and Safety of a Wound Healing Ointment with Medicinal Plant Bioactives: In Vitro and In Vivo Preclinical Evaluations

Juliana Ferreira Floriano ^{1,2,3}, Daniel Rodrigues ^{4,5}, Rie Ohara ⁶, Nara Lígia Martins de Almeida ⁷, Vanessa Soares Lara ⁷, Patricia Sartorelli ⁸, Carlos Frederico de Oliveira Graeff ⁹, Simone dos Santos Grecco ^{8,10}, Alejandra Hortencia Miranda González ^{10,11,12} and Paulo Henrique Perlatti D'Alpino ^{6,10,13,*}

¹ National Heart and Lung Institute, Imperial College London, London, UK

² São Paulo State University (UNESP), Botucatu Medical School, Botucatu, SP, Brazil

³ São Paulo State University (UNESP), School of Pharmaceutical Sciences, Araraquara, SP, Brazil

⁴ Universidade Anhanguera de São Paulo (UNIAN), Biotechnology and Innovation in Health Program, São Paulo, SP, Brazil

⁵ Fundação Nacional de Gestão de Saúde, São Paulo, SP, Brazil

⁶ Universidade Nove de Julho, Medical School, Bauru, SP, Brazil

⁷ Department of Surgery, Stomatology, Pathology and Radiology, Bauru School of Dentistry, University of São Paulo (USP), Bauru, SP, Brazil

⁸ Department of Chemistry, Institute of Environmental, Chemical and Pharmaceutical Sciences, Federal University of São Paulo, Diadema, SP, Brazil

⁹ São Paulo State University (UNESP), School of Sciences, POSMAT—Post-Graduate Program in Materials Science and Technology, Bauru, SP, Brazil

¹⁰ Triplet Biotechnology Solutions, Inc., Bauru, SP, Brazil

¹¹ Uniderp Anhanguera University, Post-Graduate Program in Dentistry, Campo Grande, MS, Brazil

¹² University of Cuiabá (UNIC), Post-Graduate Program in Integrated Dental Sciences, Cuiabá, MT, Brazil

¹³ São Paulo State University (UNESP), School of Sciences, Bauru, SP, Brazil

* Correspondence: paulodalpino@gmail.com

Abstract: Chronic wounds have a significant impact on patients' quality of life, necessitating the management of pain, infection, bleeding, and emotional challenges. Debridement, which involves the removal of nonviable tissue, is crucial for promoting wound healing. In addition to surgical methods, cost-effective alternatives such as local solutions and ointments with biological properties have been explored. The use of natural compounds with anti-inflammatory, antibacterial, and collagen-synthesizing abilities holds promise for wound healing. This study aimed to assess the safety and effectiveness of a wound-healing ointment containing bioactive ingredients derived from medicinal plants (extracts, essential oils, and vegetable oils). Pre-clinical tests were conducted following standardized protocols. The chemical composition of the ointment was characterized using Fourier transform infrared (FTIR) spectroscopy to gain insights into its synergistic action. FTIR analysis revealed similarities between the product's spectrum and that of bioactive compounds. The *in vitro* tests demonstrated that all formulations of the ointment induced no cell death, DNA damage, or acute toxicity in cell cultures. No lethal dose was observed, indicating the safety of the ointment at all concentrations. *In vivo* preclinical analyses demonstrated no adverse responses being effective in the healing process, similar to the gold standard (Silver Sulfadiazine). The regenerative ointment displayed excellent biocompatibility and bioactivity *in vitro* and *in vivo* studies, contributing to the development of innovative and sustainable wound management therapies.

Keywords: chronic wounds; wound care; natural compounds; biocompatibility; pre-clinical tests

1. Introduction

Chronic wounds can have a significant impact on quality of life, comparable to that of kidney and heart disease (Las Heras et al., 2020). These persistent wounds, caused by various conditions such as diabetes, fail to heal within a reasonable timeframe, leading to pain and disability (Chen et al., 2020). Currently, it is observed that the mortality rate of patients with chronic wounds is similar to that of patients with cancer (Sen, 2021). Chronic wounds, such as ulcers in the lower limbs, constitute a serious public health problem, affecting a large portion of the population, mainly adults and the elderly (Broughton et al., 2006). Local treatment aims to alleviate pain and itching, prevent wound infection and bleeding, and address the physical and emotional challenges associated with chronic wounds. These challenges include managing excessive exudate, which can result in unpleasant odors (Eriksson et al., 2022). Chronic wounds interfere with patients' quality of life, as well as with morbidity and mortality rates, as they produce chronic changes in skin integrity, often causing incapacitation and/or amputation of lower limbs in these individuals (Junker et al., 2013).

Chronic skin wounds can be classified, according to their etiology, into venous, arterial, mixed, and neuropathic, among others, and have their own diagnostic characteristics (Frykberg and Banks, 2015). Health professionals play a crucial role in diagnosing and distinguishing various wound types to recommend appropriate treatments. Clinical evaluation is vital for identifying intrinsic factors that impact wound healing. Moreover, numerous clinical conditions, including advanced age, diabetes mellitus, chronic renal failure, obesity, malnutrition, and connective tissue disorders, increase the risk of infection (Bowers and Franco, 2020). Each wound should be assessed individually, taking into account factors such as the time and cause of injury as well as the wound characteristics and patient factors that can influence the functional and aesthetic outcomes (Eming et al., 2014).

Debridement of the wound bed is a crucial step in facilitating enhanced wound healing (Childs and Murthy, 2017). This technique involves the partial or complete removal of nonviable tissue from the wound, aiding in the preparation of the wound bed and promoting healing (Thomas et al., 2021). By eliminating devitalized or necrotic tissues, debridement supports the regeneration of healthy tissue and improves the overall healing process (Childs and Murthy, 2017). While surgical methods are commonly used for debridement, there are cost-effective alternatives that involve prescribing associated methods, such as the application of local solutions and ointments with autolytic, enzymatic, and/or biological action, along with mechanical removal techniques like simple curettage. These approaches offer effective means to facilitate debridement without the need for extensive surgical procedures, providing more accessible options for wound treatment (Thomas et al., 2021).

In this context, there is a growing interest in exploring innovative approaches to debridement by investigating the potential of natural compounds. These compounds possess valuable properties such as anti-inflammatory, antioxidant, antibacterial, and collagen-synthesizing abilities, making them promising candidates for effective wound healing agents. This pursuit of natural compounds reflects the ongoing quest for alternative and sustainable solutions in the field of wound care, driving research and development towards novel therapeutic interventions. Numerous studies have been conducted to evaluate the efficacy of these compounds, opening new avenues for the development of novel therapies in wound management (Anuar et al., 2008; Eriksson et al., 2022; Ibrahim et al., 2018; Leite et al., 2020; Wang et al., 2018). The therapeutic effects of natural products can be attributed to the presence of bioactive phytochemical components such as alkaloids, saponins, and phenolic compounds, including flavonoids and tannins, and from essential oils (Criollo-Mendoza et al., 2023). Therefore, the aim of this *in vitro* study was to systematically assess the safety and efficacy of a wound healing ointment containing bioactives derived from medicinal plants, including extracts, essential and vegetable oils, along with other ingredients. Pre-clinical tests, including cytotoxicity, genotoxicity, and acute toxicity assessments, were conducted based on ISO 10993-3 and ISO 10993-5 (ISO10993-3, 2014; ISO10993-5, 2009). An *in vivo* preclinical test was also performed to analyze the influence of this wound healing ointment on the healing of excisional skin wounds using animal model. Additionally, by Fourier transform infrared (FTIR) spectroscopy, a physicochemical characterization of the bioactives present in the formulation and ingredients was performed to gain a comprehensive understanding of their composition and their synergistic action in the final

formulation. Both *in vitro* and *in vivo* preclinical studies confirmed the efficacy and safety profile of the tested ointment formulations, which caused no excessive cell death, membrane damage, DNA damage, or acute toxicity and caused no adverse responses, being effective in the healing process, similar to the gold standard (Silver Sulfadiazine). However, limitations exist as *in vitro* conditions and can differ from *in vivo* and clinical settings. Future research should focus on clinical studies to validate their efficacy and assess long-term effects, interactions, and clinical impact on wound healing.

2. Materials and Methods

2.1. Product Description

Pharmacure⁺ Classic Reestruturante (TAG Distribuição e Comercialização de Importados em Geral Ltda, Belo Horizonte, Brazil) is a skin wound healing ointment that contains bioactives from medicinal plants, including extracts, essential and vegetable oils, in association with other bioactive ingredients. In Table 1, the bioactives present in the product formulation are listed.

In order to assess the safety of the product, three different variations were tested according to the concentrations of bioactives, namely: PHP (standard concentration); PHP+ (three times higher bioactives than the standard); and PHP- (three times lower bioactives than the standard). The products were kept at room temperature and away from light until the moment of the study.

Table 1. Plant-based bioactives in the product formulation*.

VEGETABLE OILS
ANDIROBA OIL (CARAPA GUIANENSIS)
NEEM OIL (AZADIRACHTA INDICA)
COPAIBA OIL (COPAIFERA LANGSDORFFII)
PLANT EXTRACTS
ALOE DRIED EXTRACT (ALOE VERA)
ROSEMARY GLYCOLIC EXTRACT (ROSMARINUS OFFICINALIS)
CALENDULA GLYCOLIC EXTRACT (CALENDULA OFFICINALIS)
BARBATIMAO GLYCOLIC EXTRACT (STRYPHNODENDRON SP.)
BLEND (GLYCOLIC EXTRACTS OF CARICA PAPAYA AND ALOE VERA)**
ESSENTIAL OIL
TEA TREE (MELALEUCA ALTERNIFOLIA)
OTHER BIOACTIVES
NANO SKIN THERAPY***
HYALURONIC ACID
BLEND (GLYCOLIC EXTRACTS OF CARICA PAPAYA AND ALOE VERA)***

* Manufacturer's information. ** Pharmacure, Belo Horizonte, Brazil. ** Nanovetores Sapiens Parque, Florianópolis, Brazil.

2.2. Fourier Transform Infrared (FTIR) Spectroscopy Analysis of the Chemical Bonds

The chemical bonds present in the formulations (PHP, PHP+, and PHP-) as well as in the ingredients were analyzed using spectroscopic technique. For that, FTIR analysis was performed using an IRPrestige-21 FTIR Spectrometer (Shimadzu Corporation, Kyoto, Japan). Infrared spectra were obtained by placing each sample directly against the diamond ATR crystal. Data were collected in transmission mode using 64 scans accumulation at a resolution of 4 cm⁻¹ and wavelength ranging from 4000 to 400 cm⁻¹. All data was processed using the OriginPro 8 software. The chemical bonds were determined by comparing the recorded spectra with the standard spectral library.

2.3. Cell Culture

The NIH/3T3 strain (ATCC CRL-1658TM) was used, corresponding to mouse embryonic fibroblast cells purchased from the American Type Culture Collection (ATCC, Rockville, Maryland, USA). The NIH/3T3 strain was cultivated in DMEM culture medium (Dulbecco's Modified Eagle Medium, Gibco®, Thermo Fisher Scientific, São Paulo, Brazil) supplemented by 10% fetal bovine serum (FBS) (HyClone®, Karnataka, India) and 1% Penicillin/Streptomycin (Sigma Aldrich®, São Paulo, Brazil). Cells were observed under an inverted microscope (Olympus® CKX41, Tokyo, Japan), and the culture flask was kept in an oven at 95% relative humidity, 5% CO₂, and 37 °C (Ultra Safe® HF 212 UV model, Heal Force, China) (Oliveira et al., 2017; Piacenti-Silva et al., 2016).

2.4. Subculture and Standardization

Cell growth was monitored every 24 h using an inverted phase microscope (Olympus® CKX41, Tokyo, Japan). The culture medium was changed every 48 h to remove dead cells and nourish live cells. Fibroblasts are cells that grow in an adherence monolayer, and, after approximately 80% confluence in the culture flask, subculturing was carried out. The culture medium was discarded, and the cells were washed with 5 mL of Phosphate Buffered Saline (PBS) three times. Then, 3 mL of 0.25% trypsin solution (HyClone®, Karnataka, India) were added to the culture flask to dissociate the cells at the bottom of the flask. Afterwards, 3 mL of supplemented medium were added for trypsin inactivation. The solution was centrifuged at 1200 rpm for 5 min at 21°C. The supernatant was discarded, and the pellet was resuspended in 1 mL of medium. The fibroblasts were divided into two or more culture flasks containing 10 mL of supplemented medium until the medium was changed to create a new subculture. For standardization, after this process and the resuspension of the pellet, a 1:10 dilution was made (pellet: medium) and an aliquot of the 10 µL dilution was placed in a Neubauer chamber for cell quantification in a common optical microscope (DM4 M, Leica Microsystems, Ltda®, São Paulo, SP, Brazil) for the acquisition of 5 × 10³ cells per well, for 96-well plates, which were kept in a humid incubator for 48 h in order to guarantee the adhesion of the cells by the entire well (100% confluence).

2.5. Specimen Preparation

An aliquot (500 mg) of the wound healing ointment, considering its three different formulations (PHP, PHP+, and PHP-), was added to centrifuge tubes containing 3 mL of supplemented medium (DMEM + 10% FBS + 1% Penicillin/Streptomycin). Specimens were incubated in an oven at 95% relative humidity, 5% CO₂, and 37°C (Ultra Safe® Model HF 212 UV) for 24 h, producing, at the end of the incubation, the corresponding conditioned medium.

The conditioned medium was then diluted in a 1:1 ratio (conditioned media: supplemented media only) (Lee et al., 2013), and subsequently 200 µL of the diluted conditioned medium solutions were used in indirect contact with the cells in each of the analyses performed, constituting the experimental groups PHP, PHP+, and PHP-. The pH of each conditioned medium was measured on a universal pH strip (pH Strip, pH-fix 0–14, 100 und/pct. MN, FortLab Express). As a negative control group, supplemented DMEM medium was used (the medium group), and as a positive control, sterile distilled water was used (Water group). After 24, 48, and 72 h, the plates were washed 1x with PBS, and the XTT assay was performed according to a previous study (Bianchi et al., 2022), with modifications.

2.6. Cell Viability Assay

The study design involved the evaluation of fibroblast NIH/3T3 proliferation in indirect contact with the product by means of an XTT assay. The XTT salt, 2,3-Bis(2-methoxy-4-nitro-5-sulfophenyl)-2H-tetrazolium-5-carboxanilide, (Sigma Aldrich Inc., St. Louis, MO, USA) was dissolved in saline solution at a concentration of 1 mg/mL. Menadione, 2-Methyl-1,4-naphthoquinone (Sigma Aldrich Inc., St. Louis, MO, USA) was dissolved in acetone at a concentration of 1 mmol/L. The formed reagent, XTT/Menadione, was prepared before each assay. After the incubation time (24, 48, and 72 h) and the washing of the plates, 200 µL of XTT/Menadione were added in triplicate, and the plates

were kept in an oven at 95% relative humidity, 5% CO₂, and 37°C (Ultra Model Safe HF 212 UV) for 3 h in the dark. Afterwards, the reading was performed in a spectrophotometer (Monochromator® based on Biotek Synergy MX, Winoosky, VT, USA), and the absorbance at a wavelength of 490 nm was evaluated (Monochromator® based on Biotek Synergy MX, Winoosky, VT, USA). The percentage reduction in metabolic activity of viable cells was calculated as percentages of optical density (OD) in the wells containing the medium group (representing 100% metabolic activity). Three independent experiments were performed for each induction period. According to the international standard ISO 10993-5 [17] for quantitative *in vitro* tests, results with a reduction in cell viability greater than 70% must be considered positive for cytotoxicity.

2.7. Evaluation of % Cell Viability in Cultures Exposed to Wound Healing Ointment (XTT Analysis)

The cell proliferation assay was performed according to the ISO 10993-5 standard [17]. Briefly, 2 mm x 3 mm of each sterile sample was placed into 24-well plates. According to the protocol procedure, 1 mL of fibroblast medium was added (hereafter referred to as “extraction medium”) to each well and incubated for 24 h at 37 °C. Then, under standard cell culture conditions, 10³ cells per well were seeded in 100 µL of extraction medium. The negative control group was seeded in 100 µL of fibroblast medium. The XTT assay (Cayman Chemical, Ann Arbor, MI, USA) allowed observation of the fibroblasts’ starting condition (T0) and proliferation activity at 24 h (T1), 72 h (T2), and 7 days (T3) follow-ups at an absorbance wavelength of 490 nm. XTT tests were performed with three technical replicates.

2.8. Genotoxicity Assay—Comet Assay

To evaluate the genotoxicity of the samples, the Comet assay was used, which allows the detection of damage in the DNA of a cell. The cultured cells that remained in contact with the samples (PHP, PHP+, and PHP-) for a period of 72 h were collected and submitted to the test, which was performed under alkaline conditions according to a previously described protocol (Tice et al., 2000). For that, a volume of 5 µL of the suspension with cells was mixed with 100 µL of low melting point agarose (0.5%, Invitrogen Ltda, USA) dissolved in phosphate buffer saline (Invitrogen Ltda, USA) and spread onto microscope slides pre-coated with normal melting point agarose (1.5%, Invitrogen LTDA). The slides were immersed in a freshly prepared lysis solution consisting of 2.5 M NaCl, 100 mM ethylenediaminetetraacetic acid (EDTA, Sigma-Aldrich Co, São Paulo, Brazil), 10% dimethylsulfoxide (Merck Chemicals, Brazil), 1% Triton X-100 (Sigma-Aldrich Co.), 10 mM Tris (Sigma-Aldrich Co, São Paulo, Brazil), pH 10, for a period of 24 h. After this period, the material was washed in PBS buffer and placed in a horizontal electrophoresis tank (28 x 17.5 x 6.5 cm, Técnica Permatron Ltda, Brazil) containing alkaline buffer (0.3 M NaOH, 1 mM Na₂EDTA, pH > 13) at 4°C for 20 min.

Using the same buffer, electrophoresis was run for 20 min at an electric field strength of 1 V/cm (25 V and 300 mA). Subsequently, the slides were washed in a neutralization buffer (0.4 M Tris-HCl, pH 7.5) for 15 min, fixed for 5 min in absolute alcohol, air-dried, and stored at room temperature. The slides were stained with 50 µL of syber green and examined with a magnification of 400x in a fluorescence microscope coupled to an image analysis system (Comet II; Perspective Instruments, Suffolk, UK). The visual scoring of the comet assay was evaluated by a single person to minimize scoring variation. All slides were coded, and 50 nucleotides were randomly analyzed.

The tail intensity (amount of DNA in the comet’s tail) and the tail moment (product of tail length and the percentage of DNA in the tail) were used to measure the extent of DNA damage (Olive et al., 1990). Comet images with a „cloudy” appearance or with a very small head and balloon-like tail were excluded from the analysis (Tice et al., 2000). In addition, the early assessment of cytotoxicity was evaluated using this technique, which allows early identification of programmed cell death (apoptosis) by detecting DNA fragmentation in the cell nucleus and the genotoxic response induced by the products (PHP, PHP+, and PHP-). In this manner, this analysis demonstrates their safety in relation to possible gene mutations induced by the treatment (Netto et al., 2017).

2.9. *In Vitro* Cell Migration/Proliferation Assay

For the migration test, an *in vitro* scratch assay was used. For that, fibroblasts from NIH/3T3 were plated in a 96-well plate, and after the culture reached ~100% confluence. Then, a linear scratch, mimicking an artificial wound, was created in the cellular monolayer using a sterile 200 μ L plastic tip. The wells were then washed with sterile PBS to remove dead cells, and, subsequently, culture medium was supplemented with the products tested according to the experimental groups (PHP, PHP+, and PHP-). The well images with 4x magnification were acquired between 0, 24, 48, and 72 h, counting from the moment of the scratch, which corresponds to 0 h (Leite et al., 2020). Images of scraped areas were acquired using a fluorescence microscope coupled with a camera (model INV-100, Leica Microsystems, Ltda®, São Paulo, SP, Brazil).

Wound area recovery was measured using an image processing software (imageJ/Fiji®, NIH, USA, <https://imagej.nih.gov>). In each trial, at least three replicates were performed. A negative control was used, which was composed of only cells in culture under untreated, normal conditions (Liang et al., 2007). In addition, two positive controls (positive control 1: 1 μ M colchicine, diluted with water; positive control 2: 1 μ M colchicine, diluted with supplemented culture medium, DMEM) were used.

2.10. *In Vitro* Acute Toxicity Test—Up and Down

The IC₅₀ test, which determines the cytotoxicity of a chemical in terms of the chemical's ability to inhibit the growth of half of a population of cells, was analyzed (Kojima et al., 2023). To calculate the IC₅₀ of the experimental groups for the cytotoxicity evaluation, cells were exposed to different concentrations of the tested ointment concentrations (PHP, PHP+, and PHP-). Cytotoxicity analysis was performed according to the protocol described in item 2.5. Three replicates ($n = 3$) were performed in this test. The IC₅₀ was calculated from curves constructed by plotting cell survival (%) *vs.* bioactive concentrations (μ M). The reading values were converted to the percentage of the control (percentage cell survival). Cytotoxic effects were expressed as IC₅₀.

2.11. Wound Healing Evaluation in Rat Model of Skin Wound

The animals used in the experiment were treated according to the instructions approved by the institutional review committee (Certificate 1421/2022—CEUA, Universidade Estadual Paulista—UNESP Botucatu). Animals were never exposed to inappropriate pain. Male Sprague-Dawley rats weighing from 250 to 300 g were selected. For the study, 20 adult rats were used, from the Sprague dawley® Specific Phatogen Free (SPF) line, aged 90 days (adults), obtained from the Bioterism Center of the Multidisciplinary Center for Biological Research at the State University of Campinas (CEMIB-UNICAMP), São Paulo, Brazil. The animals underwent an acclimatization period of approximately 60 days before the start of the experiments, in which they all received water and food (Nuvilab, Nuvital® Nutrientes S/A, Paraná, Brazil) *ad libitum* and were maintained (2 animals/box) under controlled conditions of temperature (22 ± 3 °C), humidity ($50 \pm 10\%$), and light/dark cycle (12 h).

The animals were randomly distributed into 4 experimental groups: three different formulations (Group 1: PHP, Group 2: PHP+, and Group 3: PHP-) and a group (Group 4) receiving 1% silver sulfadiazine (Dermazine®, brand Cristália, expiration date: 03/2025 and batch: 22630396). Group 4 was designated the gold standard or positive control, which refers to a commercial treatment or product commonly applied in clinical practice that presents satisfactory results for the treatment of the pathology for which it is intended.

In all groups, two lesions measuring 2 cm in diameter and 5 cm apart were made on the back of the animals; the first cranial lesion, 7 cm away from their neck, received treatment with different variations of the Pharmacure+ Classic Reestruturante product or the standard gold (treated group). The second caudal lesion received no treatment other than its own blood clot (negative control). In this manner, in the same animal, both treated groups and a negative control (without treatment) were obtained in order to compare the outcomes of the ointment's action on the healing process and inflammatory response.

To perform the skin ulcer, the animals were previously anesthetized, according to the protocol approved by the ethics committee. The dorsal region was trichotomized and subsequently cleaned with povidone-iodine and saline solution after cleaning the center of the area. After depilation, the skin of each rat was demarcated by rotating the cutting edge of a 2 cm-diameter metal punch, and then the circular skin segment was resected, following the punch demarcation, deepening the incision until it exposed the dorsal muscular fascia. After performing the lesion, approximately 1 mL of each product was applied to the lesion corresponding to the treatment. The ointments were applied every 12 hours for 60 days. For post-injury analgesia, morphine was administered subcutaneously at a dose of 2.0 mg/kg every 4-6 hours for 3 consecutive days, as approved by the ethics committee.

ImageJ software version 1.50i (<https://imagej.net/ij/index.html>) was used to analyze the wound area of each animal, as reported by Masson-Meyers et al., (2020) (Masson-Meyers et al., 2020), in order to calculate the area of each wound over the experimental period. In the event of formation of erythema and bedsores, edema, bleeding, exudate, and other complications, these parameters were registered.

2.12. Histological Evaluation

Skin tissue samples from treated and untreated lesions measuring 1 cm x 1 cm from all groups studied (PHP, PHP+, PHP-, Silver Sulfadiazine—positive control, and untreated—negative control) were collected and fixed immediately after collection in 10% buffered formalin. After fixation for a minimum period of 24 h, the samples were gradually dehydrated in hydroalcoholic solutions of increasing concentrations of ethanol (70%, 95%, 100%) to remove water from the tissue. The dehydrated samples were then transferred to xylene to ensure an efficient transition to paraffin. Subsequently, the samples were infiltrated and embedded in melted paraffin, allowing the samples to be preserved and solidified, making them suitable for making ultra-thin sections. Paraffin-embedded skin tissue samples were cut into ultrathin sections (5 μ m thick) using a microtome. These sections were mounted on glass slides. Slides containing the ultrathin sections were selected for hematoxylin and eosin (HE) staining to highlight cellular structures. The slides were subsequently mounted with coverslips and prepared for microscopic analysis. Tissue specimens were fixed with buffered formaldehyde solution (Sigma-Aldrich, Jurubatuba, São Paulo, Brazil) at 3.7% (pH 7.4) for 24 h under constant agitation, dehydrated using increasing concentrations of ethanol, embedded in paraffin, and 5 μ m-thick sections were histological slides. The specimens were then stained with hematoxylin and eosin (HE) to analyze the new tissue formed as well as the advent of proliferation of inflammatory cells. The slides were analyzed using a light microscope (Axiolab, Carl Zeiss GmbH, Germany), and images were taken using an attached camera (DFC300FX, Leica Microsystems GmbH, Germany).

2.13. Collagen Content Assessment

Ultra-thin section slides were also selected for Picosirius red staining to highlight collagen fibers in the connective tissue. They were then washed and mounted with coverslips for microscopic analysis. Slides stained with HE and Picosirius red were subjected to microscopic analysis. During the analysis, the characteristics of the tissue were observed, including cellular morphology, the presence and quantification of cellular infiltrate, the presence of collagen fibers, vascularization, and any other relevant characteristics.

Collagen quantification through Picosirius red staining was performed using the open-source image processing software ImageJ. Initially, images of representative areas of the slides stained with Picosirius red were captured using a Leica DM 2500 photomicroscope with the same lighting configuration and settings for all samples. Images were then loaded into ImageJ. Subsequently, the scale was defined so that the software could calculate measurements in real units. For this measurement, the „Analyze” function in the menu and selecting „Measure” were used to calculate the area of the selection that corresponded to the collagen in the image. This action was repeated in 10 fields of each slide in different areas. After collagen quantification in all images, the data was analyzed and comparison between the experimental and control groups were obtained.

2.14. Statistical Analysis

Graphics and statistical analyses were performed with GraphPad Prism version 5 (La Jolla, CA, USA) and Statistic 10.0 (StatSoft®, Tulsa, OK, USA). The data were presented in a descriptive-representative way by means \pm SD and/or submitted to one-way or two-way ANOVA, followed by the post-hoc test of Tukey HSD (Honest Significant Difference) or the Dunn test for multiple comparisons, allowing comparison between different treatments and periods. Otherwise, the non-parametric Kruskal-Wallis test was used. The results were analyzed using parametric Student's t tests to evaluate the differences between the means between two groups (experimental x control group). ANOVA, Student's t test, and non-parametric tests were used in the statistical analysis of the collagen content. The established significance in all statistical analyses was 5%.

3. Results

3.1. Fourier Transform Infrared (FTIR) Spectroscopy Analysis of the Chemical Bonds

The bioactive spectra were grouped according to the range of their concentrations at the ointment standard formula (PHP). The exact concentration of bioactive ingredients was omitted to preserve the confidentiality of formulation. Thus, in Figure 1A, a representative spectrum of PHP and the spectra of the bioactive ingredients present in lower concentrations in the product formulation (Aloe extract, Copaiba oil, Tea tree essential oil, and Neem oil) are presented. Figure 1B illustrates the spectra of the PHP sample and the bioactive compounds present in intermediate concentrations (Hyaluronic acid, Calendula extract, Barbatimao extract, and Nano Skin Therapy). In Figure 1C, the spectra of bioactives with higher concentrations in the product formulation (Rosemary extract, Andiroba oil, and Blend) are also displayed and compared with the spectra of PHP, whereas Figure 1D illustrates the spectra of ointment samples at different concentrations of bioactives (PHP, PHP+, and PHP-). In addition, FTIR spectra show the characteristic vibration bands of samples.

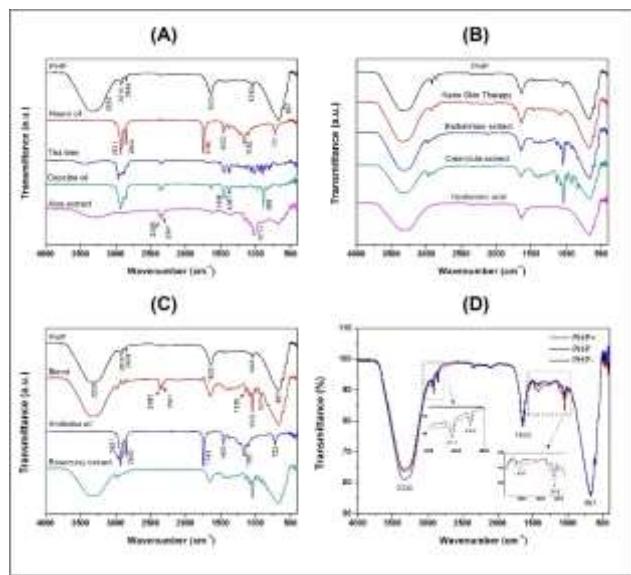


Figure 1. Representative FTIR spectra of samples: (A) PHP and bioactive ingredients ranging from 0.050 (Aloe extract) to 0.400% (Neem oil); (B) PHP and bioactive ingredients ranging from 0.500 (Hyaluronic acid) to 1.000% (Nano Skyn Therapy); (C) PHP and bioactive ingredients ranging from 1.750 (Rosemary extract) to 10.00% (Blend); (D) ointment at different concentrations of bioactives (PHP+, PHP and PHP-).

Table 2 indicates the infrared frequencies and corresponding band assignments. All spectra related to extract samples as well as Nano Skin Therapy, Hyaluronic acid, Blend, and ointment compositions showed a broad band referring to the -OH stretching between 3435 and 3280 cm^{-1} , which indicates the presence of water. It is possible to check the characteristic vibration of -CH

stretching in the region between 2979 and 2960 cm^{-1} for all extracts, except for Aloe, and Blend. The absorption bands in the 2920 cm^{-1} and 2850 cm^{-1} regions are related to the asymmetric $\nu_{\text{asy}}(\text{CH}_2)$ and symmetric $\nu_{\text{sym}}(\text{CH}_2)$ vibrations, respectively, as well as the stretching of $-\text{CH}_3$ groups. The strong absorbance band at 1743 cm^{-1} indicates that a carbonyl group ($\text{C}=\text{O}$) is present in Neem oil and Andiroba oil. Medium signals in the FTIR spectra observed in the region of 1647-1633 cm^{-1} are mainly related to the $\nu(\text{C}=\text{C})$ stretching vibration. Still, in the range of 1463-1414 cm^{-1} and 1377-1338 cm^{-1} , characteristic bands are observed representing the $\delta(\text{C}-\text{H})$ bending vibration. Another characteristic of the spectra is the presence of peaks in the region between 1181 cm^{-1} and 1015 cm^{-1} , which can be attributed to the $\nu(\text{C}-\text{O})$ stretching vibration. In the same way, the weak absorbance bands between 990 and 921 cm^{-1} , the sharp peak at 885 cm^{-1} and the intense broadbands at $\sim 667 \text{ cm}^{-1}$ are assigned to the $\delta(\text{C}=\text{C})$ bending mode. Other bands (2360 cm^{-1} and 2341 cm^{-1}) seem to be related to technical artefacts (surface moisture adsorption by the specimens and the presence of CO_2). All ointment formulations exhibited similar spectra, irrespective of the concentration of bioactives. No other peaks were observed, and this demonstrates that all samples have the same functional groups. However, the peak intensities at 2916 cm^{-1} and 2848 cm^{-1} , which are assigned to the $\nu(\text{CH}_2)$ and $\nu(\text{CH}_3)$ stretching vibrations, decrease as the concentration of bioactives decreases in the ointments. This is also observed considering the interval in the range of 1500-1000 cm^{-1} . Furthermore, some of the bands observed in the spectra of the bioactive compounds were not identified in the ointment formulations. This can probably be attributed to the low concentration of some of the bioactive compounds.

Table 2. Infrared frequencies and band assignments of PHP samples and bioactive compounds.

Wavenumber (cm^{-1})												Band assignm ent		
Bioactive compounds													Band assignm ent	
Neem oil	Tea tree	Copai ba oil	Aloe ba oil extract	Nano				Andiroba oil	Rosemary extract	PHP- y	PHP- x	PHP+ y		
				Neem oil	Tea tree	Copai ba oil	Aloe ba oil extract							
-	3435	-	3280	3350	3324	3324	3324	3312	-	3324	3335	3335	3335	v(O-H)
-	2960	-	-	-	2978	2974	2974	-	2979	-	2979	-	-	v(C-H)
2921	2914	2924	2916	2924	-	2934	-	-	2921	-	2916	2916	2914	$\nu_{\text{asy}}(\text{CH}_2)$
2852	2875	2856	-	2853	-	2880	-	2882	2852	-	2850	2850	2848	v(CH_3)
-	2360	2359	2359	-	-	-	2359	2360	-	2362	-	-	-	$\nu_{\text{sym}}(\text{CH}_2)$
-	2341	2341	2341	-	-	-	-	2341	-	-	-	-	-	v(CH_3)
-	2341	2341	2341	-	-	-	-	-	1743	-	-	-	-	v(O=C=O)
1743	-	-	-	-	-	-	-	-	1743	-	-	-	-	v(O=C=O)
-	-	1633	1633	1643	1644	1647	1633	1642	-	1644	1633	1640	1640	v(C=C)
1463	1446	1446	-	1462	-	-	-	-	1463	-	-	-	1414	$\delta(\text{C}-\text{H})$
1377	1377	1367	1338	-	-	-	-	-	1377	-	-	-	-	$\delta(\text{C}-\text{H})$
1160	-	1181	1148	-	-	-	-	-	1160	-	-	-	-	v(C-O)
-	-	-	-	-	1136	1136	-	1135	1116	1136	-	-	-	v(C-O)
-	-	-	-	1085	1081	1079	-	1079	-	1080	-	-	-	v(C-O)
-	1026	-	1015	-	1042	1040	-	1042	-	1041	1043	1043	1043	v(C-O)
-	-	967	-	-	990	990	-	990	-	-	-	-	-	$\delta(\text{C}=\text{C})$
-	-	-	-	-	921	921	-	922	-	921	-	-	-	$\delta(\text{C}=\text{C})$
-	887	885	895	-	-	837	-	-	-	-	-	-	-	$\delta(\text{C}=\text{C})$
721	-	-	-	-	-	-	-	-	722	-	-	-	-	$\delta(\text{C}=\text{C})$
-	-	-	667	667	669	667	667	667	-	669	667	666	667	$\delta(\text{C}=\text{C})$

ν = stretching vibration, ν_{asy} = asymmetric stretching, ν_{sym} = symmetric stretching, δ = bending vibration

3.2. Evaluation of % Cell Viability in Cultures Exposed to the Regenerative Ointment (XTT Analysis)

In the cell viability analysis, the negative control group (medium group) exhibited similar mean percentage values ($p > 0.05$), close to 100%, across all evaluated time periods (24, 48 and 72 h). Likewise, the positive control group (water group) displayed the lowest mean values (approximately 19%) throughout the analysis, with no significant difference between them. These findings validate the results obtained for the experimental groups, as depicted in Figures 2 and 3.

The study revealed that the regenerating ointment ensured a beneficial impact on cell viability, regardless of the experimental groups (PHP, PHP+, and PHP-), when in indirect contact with fibroblasts (NIH/3T3) for 24 h. The average cell viability percentage in the experimental groups (PHP, PHP+, and PHP-) was significantly higher compared to the negative control group (~40%). Moreover, the viability exceeded the recommended threshold of $\geq 70\%$ according to ISO 10993-5. Additionally, the experimental groups not only exhibited lower cytotoxicity but also demonstrated the ability to stimulate cell proliferation, with percentages ranging from 119.1% to 159.4% compared to the negative control group (99.8%) (Figure 2).

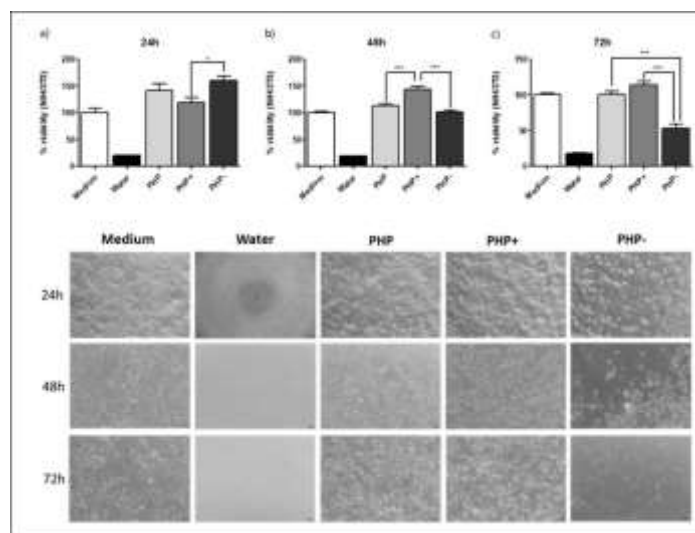


Figure 2. Percentage (%) of fibroblast viability (NIH/3T3) in indirect contact by the PHP, PHP+, and PHP- groups. The results are presented according to the mean \pm standard deviation (SD) of the percentage values obtained in the XTT viability assay in the periods of a) 24 h, b) 48 h, and c) 72 h. As a growth control, supplemented medium was used (Medium group) and as a death control, distilled water was used (Water group). Three independent experiments ($n = 5$) were performed. The statistical analysis of the data included a first evaluation of the normal distribution, followed by the one-way analysis of variance (ANOVA) following Tukey's test for multiple comparisons between groups. Below are representative images corresponding to each evaluated period (40x). It is possible to observe the cellular density in microscopic images. * $p=0.01$, and *** represents $p = 0.00$.

It is important to note that while the PHP group (with viability percentages of 140.9%, 113.1%, and 100.1% for the respective evaluation periods) and the PHP- group (with viability percentages of 159.4%, 101.3%, and 52.9% for the respective evaluation periods) showed a tendency of decreasing viability over time, reaching the lowest percentage at 72 h for the PHP- group (52.9%), the PHP+ group exhibited a significant increase in cell viability (119.1% and 143% at 24 and 48 hours, respectively) compared to the negative control and the 24-hour period of the same group ($p < 0.001$). Additionally, at 72 h, the cell viability still remained similar to that of the negative control group ($p > 0.05$), with a relative increase of 13.5% regardless of the statistical equivalence (Figure 2). Thus, PHP samples, mainly after 24 h of indirect contact (through medium conditioning) with fibroblasts, proved to be biocompatible and have relevant proliferative potential, according to this analysis.

Analyses of cell morphology performed showed adherent cells with a flattened and elongated shape, which are characteristic of viable cells. This aspect was found in cells treated with PHP, PHP+, and PHP- conditioned medium, as can be seen in the representative images of Figure 2.

3.3. Genotoxicity Assay—Comet Test

The findings from the genotoxicity study revealed that none of the tested formulations (PHP, PHP+, and PHP-) induced significant DNA damage, which can potentially trigger apoptosis or result in mutations associated with the development of diseases linked to genetic alterations (Figure 3). The observed DNA damage is within the range of normal cellular processes and can be repaired naturally. Thus, all tested formulations exhibited satisfactory results in this analysis, as the level of DNA damage was comparable to or even lower than that of the untreated negative group.

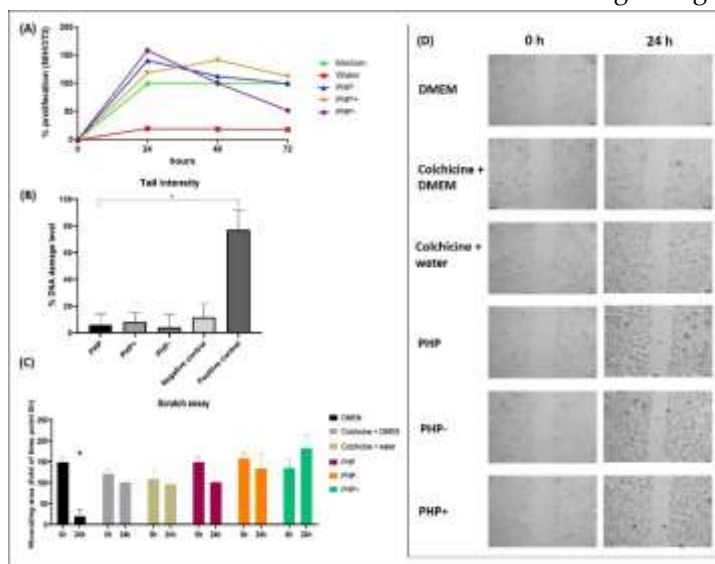


Figure 3. Evaluation of *in vitro* biocompatibility, bioactivity, and acute toxicity of the regenerative ointment. A) Fibroblast proliferation curve (NIH/3T3) compared to the PHP, PHP+, and PHP groups. In the graph, the results of the percentages (%) and average values obtained in the viability test (XTT) in periods of 24, 48, and 72 hours are plotted. As a negative control, supplemented DMEM media was used (Medium group), and as a positive control, distilled water was used (Water group). Three independent experiments were performed. The parametric quantitative results were submitted to a log-rank test to compare the proliferation curves according to the groups. * $p=0.01$; *** $p=0.00$. B) Graph with the results of the genotoxicity study evaluated by the comet assay. The graph presents the level of DNA damage (tail intensity) caused to NIH/3T3 cells in indirect contact with all tested formulations. * < 0.05 positive control, PHP; PHP+; PHP- and negative control. C and D Migration test (lesion in cell monolayer scratch assay). C) The graph demonstrates that there were no significant differences among the studied groups, only the negative control showed a greater recovery area in the 24-h period. * < 0.05 negative control vs. positive control 1 and 2; PHP+; PHP, and PHP-. D) Photomicrographs exhibit the wound healing in the cell monolayer lesion. The scale bar represents 200 μ m.

3.4. Cell Migration Assay

The migration test did not demonstrate any improvement in the wound healing of the cell monolayer lesion. All groups under study exhibited similar results, except for the negative control group, which exhibited greater recovery of the cell monolayer within 24 hours (Figure 3).

3.5. In Vitro Acute Toxicity Test—Up and Down

The cytotoxicity and genotoxicity results obtained from the evaluation of the cells in culture after 24 to 72 h of indirect contact with the conditioned medium of the three tested formulations revealed that none of the formulations exhibited cytotoxic or genotoxic effects. No lethal dose was found in

the tested formulations, so PHP, PHP+, and PHP- demonstrated safety for use in cell cultures (Figures 2 and 3). Since acute toxicity manifests within short periods (hours or days) after exposure, typically characterized by tissue breakdown or cell death, to degrees that exceed repair or adaptation of the biological system, often in these cases there is an observation of rapid lethal effects, which were not observed at any time in the *in vitro* tests performed. Conversely, the up and down test, which allows the determination of cytotoxicity (OECD 129), the results were very positive, as even an overdose of the product was not able to cause harmful effects.

3.6. Wound Healing Evaluation in Rat Model of Skin Wound

Representative images of the evolution of the closure of excisional skin wounds in animals are displayed in Figure 4. According to the observations of adverse reactions described in item 2.11, none of the treated groups presented adverse responses in the first 30 days of treatment. Therefore, no skin irritation was observed after applying the treatments during this period. However, at the end of the experiment, close to the 42nd day of treatment, slight skin irritation was observed around the treated area. The most affected animals belonged to experimental groups PHP, PHP+, and PHP-. Therefore, these adverse reactions ceased in the following week, progressing to normal skin at the end of the experiment. Regarding the local mild skin irritation around the treated area after application of formulations PHP, PHP+, and PHP-, as previously described, this reaction ceased progressing to normal skin at the end of the experiment. The observations allow us to outline some hypotheses to elucidate this effect. One of them is based on the sticky texture of the treatments used (ointments), which favors the accumulation of residues from the animal's maintenance box, especially in areas where hair has grown (areas adjacent to the lesion), due to greater adherence to the hair. This retention may have led to the "irritated" appearance that was observed at this point in the experiment. Furthermore, this ointment residue in these regions may have made trichotomy difficult, contributing to the appearance of these red-brown regions.

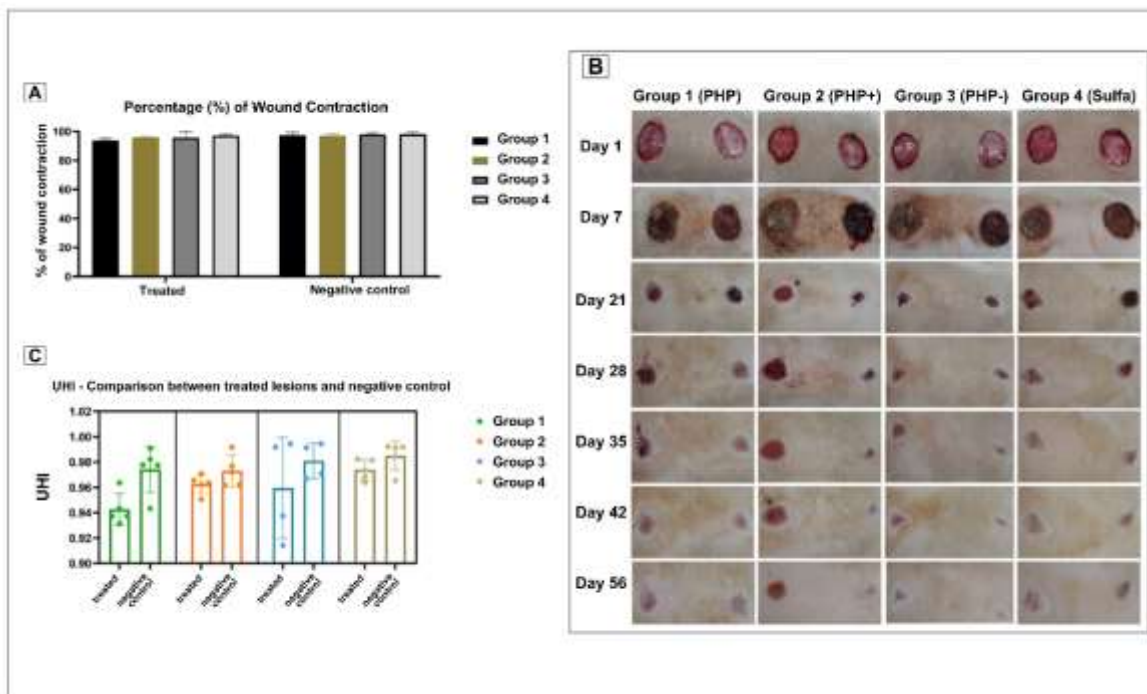


Figure 4. A) Representation of the percentage (%) of wound contraction in all groups studied, demonstrating the contraction of the treated lesion and negative control (untreated), respectively. B) Representative images of the development of the study, demonstrating the treated and untreated lesions of one animal from each group studied on days 1 (start of the study), 7, 21, 28, 35, 42, and 56 days. C) Mean UHI of the groups studied, presenting treated and untreated lesions (negative control), respectively for each group. * P<0.05.

3.7. Wound Contraction and Percentage of Contraction

The results of the percentage (%) of wound contraction in the experimental groups in the macroscopic analysis obtained in the *in vivo* preclinical study are displayed in Figure 4. It was observed that the formulations PHP, PHP+, and PHP- caused no adverse responses to the animals and were effective in regulating the healing process, similar to the control “gold standard” (Silver Sulfadiazine). Treatment with these formulations also exhibited similar contraction of the treated lesions and negative control (untreated) areas by the reduction of the ulcerated area with consequent re-epithelialization.

3.8. Ulcer Healing Index (UHI)

The results of UHI in the experimental groups in the macroscopic analysis are displayed in Figure 4. It was observed that all groups exhibited a decrease in the ulcerated area with re-epithelialization, UHI means greater than “0” (zero) was found in the experimental groups and their respective negative controls, in which “0” represents complete healing (Figure 4). In this manner, no increase was observed in the ulcerated area in all groups. The mean of Group 1- PHP was significantly different from that of its negative control group. No UHI means equal to zero were observed in the experimental groups at the 56th day, which can be attributed to less wound contraction with the re-epithelialization occurring from the base of the lesion towards the surface. In this manner, it was observed a complete healing without a drastic reduction in the area of the scar region of the wound.

3.9. Histological Evaluation

The histological analyses after 60 days revealed significant differences in the number of giant cells observed in the tissues (Figure 5). In the groups treated with PHP and PHP+, it was observed an increase of respectively 190% and 120% in the number of giant cells compared to the positive (Silver Sulfadiazine), negative control groups, and PHP-. Furthermore, a slight increase in the number of hairs and sebaceous glands, with a tendency towards a greater increase being observed in the groups treated with the formulations PHP, PHP+, and PHP- compared to the negative and positive controls (Figure 5).

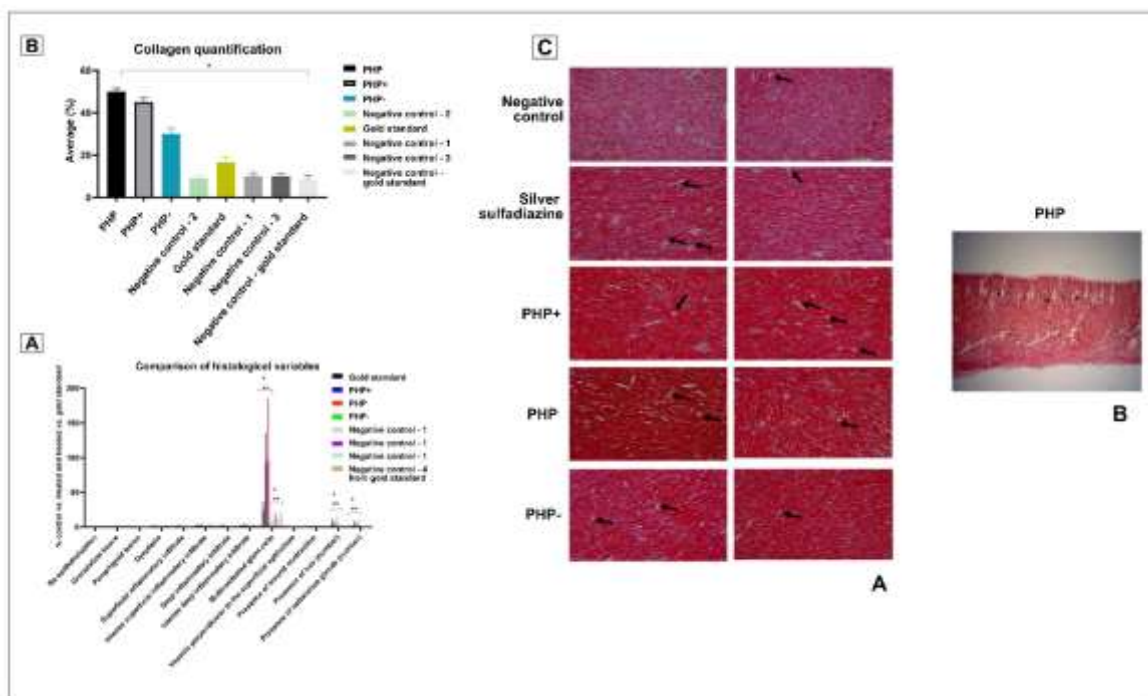


Figure 5. A) Comparison of histological variables between the treated groups (PHP+, PHP, and PHP-) and the negative control and gold standard groups (Silver Sulfadiazine). Statistical significance is indicated by * symbols for comparisons between treated vs. treated groups. negative control group and ** for comparisons between treated groups vs. the gold standard ($p<0.05$). B) Quantitative analysis of collagen carried out using ImageJ software, with presentation of the average percentage obtained. * Indicates statistical significance $p<0.05$ treated group vs. negative control group and gold standard. C) Histological plates from the study groups stained with Picosirius red, where the variation in the intensity of the reddish coloring is visible, related to the amount of collagen (indicated in red in image A) In image B, a histological slide from the PHP group is shown, with the “**” representing blood vessels perpendicular to the surface of the tissue, one of the evaluated variables that was shown to be increased in the study, although without significant differences between the groups. The arrows demonstrate the presence of giant cells in the tissue. 20X magnification.

Other variables studied, such as re-epithelialization, granulation tissue, pemphigoid lesion, dysplasia, superficial type inflammatory infiltrate (Sup type), deep type inflammatory infiltrate (Prof type), intense deep inflammatory infiltrate (Prof intens), vessels perpendicular to the surface epithelium, and presence of wound contraction exhibited no significant differences among the experimental groups (PHP, PHP+, PHP-, Silver Sulfadiazine, positive and negative control groups) (Figure 5).

3.10. Collagen Content Assessment

Regarding collagen quantification, the analysis revealed that lesions treated with PHP showed a significant difference compared to the control untreated group ($p < 0.05$), with a five-fold increase in the amount of collagen. When compared to the gold standard control group (Silver Sulfadiazine), a significant difference was also observed, whereas lesions treated with PHP treatment exhibited three times more collagen. Furthermore, collagen in this group was notably more organized compared to all groups analyzed (Figure 5). Similarly, the group treated with PHP+ also exhibited a significant increase in the amount of collagen, with an increase of 4.5 times compared to the negative control groups and 2.7 times in relation to the gold standard-positive control group (Figure 5). Although the group PHP- exhibited a smaller increase in the amount of collagen compared to other variations of the product Pharmacure+ Classic Reestruturante, it was observed that 3 times more collagen was observed compared to the negative control group and 1.8 times higher compared to the gold standard control group (Figure 5).

Discussion

The investigation of natural compounds possessing anti-inflammatory, antioxidant, antibacterial, and collagen-synthesizing properties has shown promise in the field of wound healing (Ibrahim et al., 2018). The utilization of natural compounds offers several advantages over conventional approaches. Firstly, natural compounds are often readily available and can be obtained from various plant sources (Yuan et al., 2016). This accessibility contributes to their potential cost-effectiveness, making them viable options for widespread application in healthcare settings (Jeon et al., 2011). Additionally, natural compounds have demonstrated diverse biological activities, including anti-inflammatory effects that can help alleviate the inflammatory response associated with wound healing (Criollo-Mendoza et al., 2023). By reducing inflammation, natural compounds may promote a more favorable environment for the healing process to proceed (Criollo-Mendoza et al., 2023). Considering the sequential nature of the wound healing process and the intended use of the tested product, it is reasonable to expect that the natural bioactives compounds in combination with other compounds present in the formulation would exert their biological effects in alignment with the different phases of healing.

The healing process comprises three phases: hemostasis and inflammation; proliferation; and remodeling and maturation (Wang et al., 2018). In this context, for the hemostasis phase, when coagulation, platelet proliferation, expression of growth factors, cytokines, immunomodulation,

collagen degradation, and edema formation occur, it is expected that the synergic biological effects of the vegetable oils (andiroba and copaiba), the essential oil of *Melaleuca alternifolia*, the plant extracts of *Carica papaya*, *Rosmarinus officinalis*, and *Stryphnodendron sp.*, together with those of Nano Skin Therapy and hyaluronic acid (Alves et al., 2019; Andrade et al., 2018; Gushiken et al., 2017; Lima et al., 1998; Pazyar et al., 2014; Yogiraj et al., 2014). Nano Skin Therapy is a commercial product with a blend of bioactives from *Curcuma aromatica*, *Rosa aff rubiginosa*, and *Aloe vera* plant extracts nanoencapsulated in lipid particles with a diameter ≥ 200 nm. Nanoencapsulation allows the stabilization of sensitive and complex components that are highly soluble in water. These plant-based bioactives are also indicated for wound care (Berlanga-Acosta et al., 2009; Dosoky and Setzer, 2018; Liang et al., 2021).

Another ingredient in the formulation in the so called "blend", which is composed of glycolic extracts of *Carica papaya* and *Aloe vera*. Aqueous propylene glycol extracts from medicinal plants are commonly used as active ingredients in the production of medicine and beauty products for external application (Volkov et al., 2021). Glycols are solvents used as extraction agents in the extraction of biologically active compounds from hydrophilic plant extracts (Volkov et al., 2021). It also acts as a carrier, enhancing the targeted delivery of natural ingredients. Glycols are used as humectants, reducing water activity, thus enhancing their preservative effect and allowing a long shelf life (Padmawar and Bhadoriya, 2018). As bioactive ingredients, it is expected that these two glycolic extracts would present an enzymatic action in the wound prior to the granulation phase, helping in the formation of new scar tissue (Anuar et al., 2008; Liang et al., 2021).

In the proliferation phase, all the bioactives seem to act, whether in the proliferation of fibroblasts, collagen synthesis, angiogenesis, re-epithelialization, formation of granulation tissue, and wound contraction. Finally, in the remodeling phase and maturation of the scar tissue, it is expected that the copaiba oil, the plant extracts of *Aloe vera*, *Rosmarinus officinalis*, and *Stryphnodendron sp.*, the essential oil of Tea tree, and Nano Skin Therapy act: inducing re-epithelialization, remodeling of collagen III to collagen I, stimulating the action of metalloproteinases, remodeling of fibroblasts to myofibroblasts, proliferation of keratinocytes, deposition of permanent extracellular matrix, and organization of the collagen fibers (Andrade et al., 2018; Edmondson et al., 2011; Liang et al., 2021; Lima et al., 1998; Pinto et al., 2023). It is important to mention that at the "blend", specifically at papaya glycolic extract, can be found glycolic papain, which has an enzymatic action on the wound prior to the granulation phase, helping the formation of new scar tissue (Hakim et al., 2019). Another component to highlight is high-molecular-weight hyaluronic acid, which has the function of hydrating the wound and contributing to a humid microenvironment that also favors the formation of collagen (Yang et al., 2021).

Overall, the FTIR spectra analysis presented in Figure 1 provides valuable information about the chemical composition, interactions, and potential synergistic effects of the product and its ingredients. This understanding is crucial for the development and optimization of effective and safe therapeutic formulations. Further studies and characterization techniques can build upon these findings to explore the functional implications of these chemical interactions and their impact on the product's performance. The obtained FTIR spectra provide valuable insights into the composition and characteristics of the PHP product and its bioactive components. The spectra presented in Figure 1 demonstrated the variations in the vibrational bands across different concentrations of bioactives and bioactive samples. The assignment of infrared frequencies and corresponding band assignments in Table 2 further aids in understanding the molecular bonds present in the samples.

The spectrum of bioactive ingredients and ointment formulations exhibits several characteristic absorption peaks that are strongly affected by its physical and chemical structures (Du et al., 2023). For the FTIR spectrum of the PHP product, there is a broadband at 3335 cm^{-1} . This band is assigned to the hydroxyl groups (-OH) stretching vibrations. At 2916 cm^{-1} and 2850 cm^{-1} two weak bands associated with the asymmetric and symmetric C-H stretching vibrations of CH_2 , respectively, and CH_3 groups are observed. At 1640 cm^{-1} an absorption band related to the $\nu(\text{C}=\text{C})$ stretching vibration is present. The weak band at 1043 cm^{-1} refers to the $\nu(\text{C}-\text{O})$ stretching vibration. At 666 cm^{-1} , an intense broadband is attributed to the $\delta(\text{C}=\text{C})$ bending mode.

Interestingly, all PHP samples exhibit similar spectra, regardless of the concentration of bioactives, indicating the presence of the same functional groups. However, the peak intensities at 2916 cm^{-1} and 2848 cm^{-1} , corresponding to the $\nu(\text{CH}_2)$ and $\nu(\text{CH}_3)$ stretching vibrations, decrease as the concentration of bioactives decreases in PHP. This trend is also observed within the range of $1500\text{--}1000\text{ cm}^{-1}$. Furthermore, certain bands observed in the spectra of bioactive compounds are not identified in the PHP samples, likely due to the lower concentration of some bioactive compounds. These results provide valuable information about the molecular composition and structural variations in the PHP product and its bioactive components at different concentrations. Therefore, FTIR method may yield richly structured “fingerprint” spectra relating to structure and conformation (German et al., 2006; Holman et al., 2000). To summarize, FTIR is a method with many advantages (easy preparation for analysis and precision in determinations). It can be efficiently used to identify chemical compounds by recognizing their structure (Koczoń et al., 2023). However, further investigations are necessary to explore the implications of these variations and their potential impact on the efficacy and functionality of the ointment tested.

Virtually all plant-based bioactives in the formulation are able to synergistically act, either by stimulating, regulating, or inhibiting in different ways the complex and dynamic processes supported by countless cellular events, coordinated to effectively repair damaged tissue (Liu et al., 2022). The exploration of natural compounds with anti-inflammatory, antioxidant, antibacterial, and collagen-synthesizing properties, in addition to the proteolytic enzyme effect of papain, represents a promising avenue for advancing wound healing strategies. The integration of these compounds into local solutions and ointments offers a cost-effective and accessible approach to wound care. However, further research is needed to elucidate the specific mechanisms of action, optimal formulations, and clinical efficacy of these natural compounds in wound healing. Continued investigation in this field holds the potential to revolutionize wound care practices and improve patient outcomes. The present study aimed to investigate the potential therapeutic effects of a regenerating ointment containing natural compounds *in vitro*, providing valuable insights for further research and development in wound care. The results demonstrated that the ointment positively influenced cell viability, exceeding the recommended threshold of 70% according to ISO 10993-5 guidelines (Figure 2). Notably, all tested formulations, including PHP, PHP+, and PHP-, exhibited no cytotoxicity or genotoxicity (Figures 2 and 3B). The genotoxicity study revealed that none of the formulations caused significant DNA damage or programmed cell death. The observed DNA damage levels were within the range of normal cellular processes that can undergo repair. These findings suggest that the tested formulations are safe for use in living organisms, as their effects on cell cultures did not induce excessive cell death, membrane damage, or DNA damage. Moreover, the experimental groups stimulated the cell proliferative capacity (Figures 2 and 3B).

To further evaluate the safety profile of the regenerating ointment, an *in vitro* adaptation of the Up and Down test was conducted to simulate different doses administered in cell cultures (Fig. 2 and 3). In the present study, an *in vitro* study was used as an alternative method for the median lethal dose (LD) test, contributing to the reduction and refinement of the use of animals in research. In this sense, it was used as an adaptation of the test, simulating different doses administered in cell cultures (*in vitro*). The results showed that even the highest tested dose did not induce acute lethal effects in cell cultures. These results are encouraging, as they demonstrate the absence of harmful effects even at high doses, supporting the safety of the regenerating ointment.

Several medical approaches and therapeutic interventions can act on the different processes involved in the healing cascade by decreasing healing time, modifying inflammation, and accelerating the proliferative phase. In addition, some of these approaches can stimulate and optimize the remodeling phase, promoting more efficient recruitment of fibroblasts and collagen deposition (Santos et al., 2023; Song et al., 2016). Therefore, considering that wound care represents a prominent clinical area among the different pathologies and is of great clinical importance, the correct treatment and management positively influence the course of healing, reducing the potential for complications. In this manner, the development of new products for wound care is of great importance and brings countless benefits to patients, reducing costs in public health, and considerably improving the quality

of life. The results of this *in vitro* study demonstrated that Pharmacure+ Classic Reestruturante is safe, with no cytotoxic or genotoxic effects, and also enhances proliferative potential in cultured cells (Figure 3A and 3B), irrespective of its concentration.

Although the scratch migration tests did not reveal significant differences in wound closure in the cell monolayer between the ointment formulations (Figure 3C and 3D), the presence of PHP+ composition appeared to induce wound opening, indicating its potential for effective debridement. It is worth noting that the lack of observed differences in the closure of the cell monolayer lesion reinforces the limitations of the *in vitro* scratch assay, which fails to replicate the intricate dynamics of a complete tissue composed of diverse cells that respond differently during the wound healing process.

Considering the wound contraction and percentage of contraction, no significant differences were observed between the experimental groups nor between the comparison of the treated groups with the negative control group. This fact is due to differential healing, where re-epithelialization occurred from the base of the lesion to the surface without there being a high contraction of the lesion. Although the absence of significance in the statistical analysis, the negative control group (untreated group) presented a slightly increased in wound contraction, which can be observed in Figure 4. Still, considering the results of group 4 (positive control silver sulfadiazine), no wound contraction was observed as expected, and this fact needs to be investigated by studying the systemic release of the active ingredients in the treatments used as well as their pharmacokinetics in the animal's bodies. In this manner, it can be speculated that the systemic release of the active ingredients delivered in the treatment might contribute to less wound contraction than normal in untreated groups (negative control).

These results indicate that the histological and morphological variables analyzed were not affected by treatment with the different products and concentrations used. Therefore, regarding these specific characteristics, the treated groups demonstrated no significant improvement compared to the negative control groups. This lack of differences suggests that the treatment had no direct impact on re-epithelialization, the formation of granulation tissue, the presence of pemphigoid lesions, the occurrence of dysplasia, the types and intensity of inflammatory infiltrate, the formation of vessels perpendicular to the superficial epithelium, or wound contraction. It is important to note that, although these variables presented no significant differences, they may play relevant roles in other aspects of the skin healing process. Therefore, it is essential to consider that the assessment of treatment efficacy must consider not only these isolated parameters but also other relevant clinical and biological results to obtain a complete picture of the therapeutic impact on the skin's healing and regeneration processes.

The significant increase in blood vessels perpendicular to the tissue surface indicates a response to the inflammatory or infectious process. However, it is important to note that no significant differences were identified between the groups studied in this aspect. This result suggests that although there was an increase in the formation of perpendicular vessels as part of the response to infection or inflammation (Figure 5B), this change was not exclusive to any specific treatment group, which may indicate that treatment with the different formulations of the product Pharmacure+ Classic Reestruturante (PHP, PHP+, or PHP-) had no direct impact in this aspect. Therefore, other factors may be influencing this observed vascular response. It is important to further investigate these differences to understand the underlying mechanisms.

The correlation between collagen types and skin regeneration is fundamental in the context of developing new treatments to accelerate and stimulate skin regeneration (Benito-Martínez et al., 2022). Collagen plays an essential role in the structure and function of the skin, being the main component of the extracellular matrix. There are several types of collagen, with type I collagen being the most abundant in the skin and playing a crucial role in maintaining tissue integrity and resistance (Harsha and Brundha, 2020; Mathew-Steiner et al., 2021). In the skin regeneration process, the formation and adequate organization of collagen are critical to ensuring the functional restoration of the tissue. Different types of collagen can play specific roles in skin healing and regeneration. For example, type III collagen is most commonly found in the initial phase of healing, while type I

collagen is predominant in the remodeling phase (Harsha and Brundha, 2020). Therefore, analyses of the types of collagen present in skin tissue, their organization, and their relative proportions are necessary to understand how these factors affect skin regeneration. This allows the development of specific treatments that aim to modulate collagen synthesis and organization to optimize the regeneration process. Understanding the relationships between collagen types and skin regeneration is crucial for the development of innovative therapies that promote more effective and aesthetic skin recovery after injuries, traumas, or medical procedures.

The increase in giant cells promoted by the treatment may be beneficial for accelerating the regeneration process due to their specialized function in the phagocytosis of foreign material and the removal of necrotic tissues. These cells are capable of cleaning the area of injury from cellular debris, bacteria, and waste, facilitating a cleaner environment conducive to tissue regeneration (Biglari et al., 2019). Furthermore, giant cells can secrete growth factors and cytokines that stimulate cell proliferation and angiogenesis, contributing to the rapid repair of damaged tissue. Therefore, the increase in these cells at the site of injury may play a crucial role in improving the skin's healing and regeneration processes (Lorenz and Longaker, 2003; Wilgus, 2008).

The results of the present *in vivo* preclinical study indicated not only the restructuring of the skin after injury but also the formation of complex appendages, such as hair and sebaceous glands, which play a crucial role in recovering the function of the regenerated tissue (Strecker-McGraw et al., 2007). This increase in the presence of giant cells and the formation of attachments suggests a more effective response in the process of removing cell debris and necrotic tissues, which contributes to a healthier and pinker appearance of the wound bed in the groups treated with the product in comparison with the negative and positive control groups. Therefore, histological analyses corroborate the macroscopic findings and reinforce the effectiveness of the treatment in promoting healing and regeneration of skin tissue. These results indicate that PHP, PHP+, and PHP- formulations appear to play a positive role in stimulating collagen production, a fundamental component in skin regeneration and healing. Organized collagen, especially evident in the PHP group, is a promising finding, as it suggests that this treatment not only increases the amount of collagen but also contributes to its adequate organization, which is essential for the structural and functional integrity of tissues (Benito-Martínez et al., 2022). This collagen analysis supports the effectiveness of treatments with the Pharmacure+ Classic Reestruturante product (PHP, PHP+, and PHP-) in promoting skin regeneration and improving the quality of scar tissue.

While this *in vitro* study demonstrated the safety and enhanced proliferative potential of the regenerating ointment, further investigations are warranted to confirm its effectiveness and safety in clinical studies. Future studies should focus on evaluating the regenerating ointment's efficacy in promoting wound healing in human subjects. The data obtained from clinical studies will provide valuable insights into the therapeutic potential of the wound healing ointment and its applicability in clinical settings.

The exploration of natural compounds with specific biological properties represents a promising approach for advancing wound healing strategies. The *in vitro* and *in vivo* preclinical evaluations of the regenerating ointment demonstrated its safety and potential to enhance cell viability and proliferation. These findings provide a foundation for further research and development of the regenerating ointment, with the ultimate goal of improving wound care practices and patient outcomes.

4. Conclusions

Based on the findings of this *in vitro* and *in vivo* preclinical study, it can be concluded that all tested ointment formulations exhibited a favorable safety profile without inducing excessive cell death or membrane damage, as indicated by the cytotoxicity test results. Furthermore, the genotoxicity test revealed that the formulations did not elicit significant DNA damage, ruling out the potential for mutations or apoptosis within the studied period. The *in vitro* acute toxicity test provided additional evidence supporting the safety of the tested formulations. None of the formulations demonstrated high mortality rates in the cells when exposed for short durations

(minutes or hours). Moreover, even when administered at excessive doses, the tested product induced no acute adverse effects on the cell cultures, including excessive cell death, alterations in cell morphology, plastic adhesion, or growth. These findings collectively suggest that the tested ointment formulations possess a high degree of biocompatibility and pose no immediate cytotoxic, genotoxic, or acute toxic risks. Morphological analysis demonstrated that the PHP, PHP+, and PHP- caused no adverse responses and were effective in the healing process, similar to Silver Sulfadiazine, reducing the ulcerated area with re-epithelialization. Different formulations also led to healing with a lower rate of contraction, which may cause less wound contraction and scar formation and, consequently, a more homogeneous skin. Future investigations should focus on conducting clinical studies to validate the safety and efficacy of these ointment formulations. Additional research is also warranted to assess their long-term effects, potential interactions with other wound healing processes, and overall clinical impact. The orchestrated and complex nature of this biological action necessitates further investigation. By expanding our understanding of these formulations through comprehensive studies, we can ensure their suitability for clinical application and improve patient outcomes in the field of wound care.

Data availability: Data will be made available on request.

Acknowledgments: The authors are grateful for Bauru Dental School, University of São Paulo (FOB-USP), São Paulo State University (UNESP), School of Sciences, Bauru, and Nanotechnology Research Center (CPnano) for the technical support.

References

1. Alves, A.Q., da Silva, V.A.J., Góes, A.J.S., Silva, M.S., de Oliveira, G.G., Bastos, I.V.G.A., de Castro Neto, A.G., Alves, A.J., 2019. The fatty acid composition of vegetable oils and their potential use in wound care. *Adv Skin Wound Care* 32(8), 1-8.
2. Andrade, J.M., Faustino, C., Garcia, C., Ladeiras, D., Reis, C.P., Rijo, P., 2018. *Rosmarinus officinalis* L.: an update review of its phytochemistry and biological activity. *Future Sci OA* 4(4), FSO283.
3. Anuar, N.S., Zahari, S.S., Taib, I.A., Rahman, M.T., 2008. Effect of green and ripe *Carica papaya* epicarp extracts on wound healing and during pregnancy. *Food Chem Toxicol* 46(7), 2384-2389.
4. Benito-Martínez, S., Pérez-Köhler, B., Rodríguez, M., Izco, J.M., Recalde, J.I., Pascual, G., 2022. Wound Healing Modulation through the Local Application of Powder Collagen-Derived Treatments in an Excisional Cutaneous Murine Model. *Biomedicines* 10(5), 960.
5. Berlanga-Acosta, J., Gavilondo-Cowley, J., López-Saura, P., González-López, T., Castro-Santana, M.D., López-Mola, E., Guillén-Nieto, G., Herrera-Martínez, L., 2009. Epidermal growth factor in clinical practice – a review of its biological actions, clinical indications and safety implications. *Int Wound J* 6(5), 331-346.
6. Bianchi, S., Bernardi, S., Simeone, D., Torge, D., Macchiarelli, G., Marchetti, E., 2022. Proliferation and morphological assessment of human periodontal ligament fibroblast towards bovine pericardium membranes: an in vitro study. *Materials* 15(23), 8284.
7. Biglari, S., Le, T.Y.L., Tan, R.P., Wise, S.G., Zambon, A., Codolo, G., De Bernard, M., Warkiani, M., Schindeler, A., Naficy, S., Valtchev, P., Khademhosseini, A., Dehghani, F., 2019. Simulating inflammation in a wound microenvironment using a dermal wound-on-a-chip model. *Advanced Healthcare Materials* 8(1), 1801307.
8. Bowers, S., Franco, E., 2020. Chronic wounds: evaluation and management. *Am Fam Physician* 101(3), 159-166.
9. Broughton, G.I., Janis, J.E., Attinger, C.E., 2006. The basic science of wound healing. *Plast Reconstr Surg* 117(7S), 12S-34S.
10. Chen, H., Cheng, Y., Tian, J., Yang, P., Zhang, X., Chen, Y., Hu, Y., Wu, J., 2020. Dissolved oxygen from microalgae-gel patch promotes chronic wound healing in diabetes. *Sci Adv* 6(20), eaba4311.
11. Childs, D.R., Murthy, A.S., 2017. Overview of wound healing and management. *Surg Clin North Am* 97(1), 189-207.
12. Criollo-Mendoza, M.S., Contreras-Angulo, L.A., Leyva-López, N., Gutiérrez-Grijalva, E.P., Jiménez-Ortega, L.A., Heredia, J.B., 2023. Wound healing properties of natural products: mechanisms of action. *Molecules* 28(2), 598.

13. Dosoky, N.S., Setzer, W.N., 2018. Chemical composition and biological activities of essential oils of Curcuma species. *Nutrients* 10(9), 1196.
14. Du, P., Chen, X., Chen, Y., Li, J., Lu, Y., Li, X., Hu, K., Chen, J., Lv, G., 2023. In vivo and in vitro studies of a propolis-enriched silk fibroin-gelatin composite nanofiber wound dressing. *Heliyon* 9(3), e13506.
15. Edmondson, M., Newall, N., Carville, K., Smith, J., Riley, T.V., Carson, C.F., 2011. Uncontrolled, open-label, pilot study of tea tree (*Melaleuca alternifolia*) oil solution in the decolonisation of methicillin-resistant *Staphylococcus aureus* positive wounds and its influence on wound healing. *Int Wound J* 8(4), 375-384.
16. Eming, S.A., Martin, P., Tomic-Canic, M., 2014. Wound repair and regeneration: mechanisms, signaling, and translation. *Sci Transl Med* 6(265), 265sr266-265sr266.
17. Eriksson, E., Liu, P.Y., Schultz, G.S., Martins-Green, M.M., Tanaka, R., Weir, D., Gould, L.J., Armstrong, D.G., Gibbons, G.W., Wolcott, R., Olutoye, O.O., Kirsner, R.S., Gurtner, G.C., 2022. Chronic wounds: treatment consensus. *Wound Repair Regen* 30(2), 156-171.
18. Frykberg, R.G., Banks, J., 2015. Challenges in the treatment of chronic wounds. *Adv Wound Care* 4(9), 560-582.
19. German, M.J., Hammiche, A., Ragavan, N., Tobin, M.J., Cooper, L.J., Matanhelia, S.S., Hindley, A.C., Nicholson, C.M., Fullwood, N.J., Pollock, H.M., Martin, F.L., 2006. Infrared spectroscopy with multivariate analysis potentially facilitates the segregation of different types of prostate cell. *Biophys J* 90(10), 3783-3795.
20. Gushiken, L.F.S., Hussni, C.A., Bastos, J.K., Rozza, A.L., Beserra, F.P., Vieira, A.J., Padovani, C.R., Lemos, M., Polizello Junior, M., Silva, J.J.M.d., Nóbrega, R.H., Martinez, E.R.M., Pellizzon, C.H., 2017. Skin wound healing potential and mechanisms of the hydroalcoholic extract of leaves and oleoresin of *Copaifera langsdorffii* Desf. Kuntze in rats. *Evid Based Complement Alternat Med* 2017, 6589270.
21. Hakim, R.F., Fakhrurrazi, Dinni, 2019. Effect of *Carica papaya* extract toward incised wound healing process in mice *musculus* clinically and histologically. *Evid Based Complement Alternat Med* 2019, 8306519.
22. Harsha, L., Brundha, M.P., 2020. Role of collagen in wound healing. *Drug Invention Today* 13(1), 55-57.
23. Holman, H.-Y.N., Martin, M.C., Blakely, E.A., Bjornstad, K., Mckinney, W.R., 2000. IR spectroscopic characteristics of cell cycle and cell death probed by synchrotron radiation based Fourier transform IR spectromicroscopy. *Biopolymers* 57(6), 329-335.
24. Ibrahim, N.I., Wong, S.K., Mohamed, I.N., Mohamed, N., Chin, K.-Y., Ima-Nirwana, S., Shuid, A.N., 2018. Wound healing properties of selected natural products. *Int J Environ Res Public Health* 15(11), 2360.
25. ISO10993-3, 2014. Biological evaluation of medical devices, Part 3: Tests for genotoxicity, carcinogenicity and reproductive toxicity. International Organization for Standardization, Geneva, Switzerland.
26. ISO10993-5, 2009. Biological evaluation of medical devices, Part 5: Tests for in vitro cytotoxicity. International Organization for Standardization, Geneva, Switzerland, p. 34.
27. Jeon, J.G., Rosalen, P.L., Falsetta, M.L., Koo, H., 2011. Natural products in caries research: current (limited) knowledge, challenges and future perspective. *Caries Res* 45(3), 243-263.
28. Junker, J.P.E., Caterson, E.J., Eriksson, E., 2013. The microenvironment of wound healing. *Arch Craniofac Surg* 24(1), 12-16.
29. Koczon, P., Hołaj-Krzak, J.T., Palani, B.K., Bolewski, T., Dąbrowski, J., Bartyzel, B.J., Gruczyńska-Sękowska, E., 2023. The analytical possibilities of FT-IR spectroscopy powered by vibrating molecules. *Int J Mol Sci* 24(2), 1013.
30. Kojima, H., Nakada, T., Yagami, A., Todo, H., Nishimura, J., Yagi, M., Yamamoto, K., Sugiyama, M., Ikarashi, Y., Sakaguchi, H., Yamaguchi, M., Hirota, M., Aizawa, S., Nakagawa, S., Hagino, S., Hatao, M., 2023. A step-by-step approach for assessing acute oral toxicity without animal testing for additives of quasi-drugs and cosmetic ingredients. *Curr Res Toxicol* 4, 100100.
31. Las Heras, K., Igartua, M., Santos-Vizcaino, E., Hernandez, R.M., 2020. Chronic wounds: current status, available strategies and emerging therapeutic solutions. *J Control Release* 328, 532-550.
32. Lee, S.-J., Chung, J., Na, H.-S., Park, E.-J., Jeon, H.-J., Kim, H.-C., 2013. Characteristics of novel root-end filling material using epoxy resin and Portland cement. *Clin Oral Investig* 17(3), 1009-1015.
33. Leite, M.N., Leite, S.N., Caetano, G.F., Andrade, T.A.M., Fronza, M., Frade, M.A.C., 2020. Healing effects of natural latex serum 1% from *Hevea brasiliensis* in an experimental skin abrasion wound model. *An Bras Dermatol* 95(4), 418-427.

34. Liang, C.-C., Park, A.Y., Guan, J.-L., 2007. In vitro scratch assay: a convenient and inexpensive method for analysis of cell migration in vitro. *Nat Protoc* 2(2), 329-333.
35. Liang, J., Cui, L., Li, J., Guan, S., Zhang, K., Li, J., 2021. Aloe vera: a medicinal plant used in skin wound healing. *Tissue Eng Part B Rev* 27(5), 455-474.
36. Lima, J.C.S., Martins, D.T.O., de Souza Jr., P.T., 1998. Experimental evaluation of stem bark of *Stryphnodendron adstringens* (Mart.) Coville for antiinflammatory activity. *Phytotherapy Research* 12(3), 218-220.
37. Liu, E., Gao, H., Zhao, Y., Pang, Y., Yao, Y., Yang, Z., Zhang, X., Wang, Y., Yang, S., Ma, X., Zeng, J., Guo, J., 2022. The potential application of natural products in cutaneous wound healing: A review of preclinical evidence. *Front Pharmacol* 13.
38. Lorenz, H.P., Longaker, M.T., 2003. Wounds: Biology, Pathology, and Management, in: Li, M., Norton, J.A., Bollinger, R.R., Chang, A.E., Lowry, S.F., Mulvihill, S.J., Pass, H.I., Thompson, R.W. (Eds.), *Essential Practice of Surgery: Basic Science and Clinical Evidence*. Springer New York, New York, NY, pp. 77-88.
39. Masson-Meyers, D.S., Andrade, T.A.M., Caetano, G.F., Guimaraes, F.R., Leite, M.N., Leite, S.N., Frade, M.A.C., 2020. Experimental models and methods for cutaneous wound healing assessment. *International Journal of Experimental Pathology* 101(1-2), 21-37.
40. Mathew-Steiner, S.S., Roy, S., Sen, C.K., 2021. Collagen in wound healing. *Bioengineering* 8(5), 63.
41. Netto, A.O., Gelati, R.B., Serrano, R.G., Volpato, G.T., Vieira, M., Rudge, C., Damasceno, C., 2017. Approaches of whole blood thawing for genotoxicity analysis in rats. *J. Toxicol. Pharmacol* 1(007).
42. Olive, P.L., Banáth, J.P., Durand, R.E., 1990. Heterogeneity in radiation-induced DNA damage and repair in tumor and normal cells measured using the „comet” assay. *Radiat Res* 122(1), 86-94.
43. Oliveira, F.A.d., Matos, A.A., Matsuda, S.S., Buzalaf, M.A.R., Bagnato, V.S., Machado, M.A.d.A.M., Damante, C.A., Oliveira, R.C.d., Peres-Buzalaf, C., 2017. Low level laser therapy modulates viability, alkaline phosphatase and matrix metalloproteinase-2 activities of osteoblasts. *J Photochem Photobiol B, Biol* 169, 35-40.
44. Padmawar, A.R., Bhadriya, U., 2018. Glycol and glycerin: pivotal role in herbal industry as solvent/co-solvent. *World J Pharm Res* 4(5), 153-155.
45. Pazyar, N., Yaghoobi, R., Rafiee, E., Mehrabian, A., Feily, A., 2014. Skin Wound Healing and Phytomedicine: A Review. *Skin Pharmacol* 27(6), 303-310.
46. Piacenti-Silva, M., Matos, A.A., Paulin, J.V., Alavarce, R.A.d.S., de Oliveira, R.C., Graeff, C.F., 2016. Biocompatibility investigations of synthetic melanin and melanin analogue for application in bioelectronics. *Polym Int* 65(11), 1347-1354.
47. Pinto, E.P., Menezes, R.P., de S. Tavares, W., Ferreira, A.M., Sousa, F.F.O.d., Araújo da Silva, G., Zamora, R.R.M., Araújo, R.S., de Souza, T.M., 2023. Copaiba essential oil loaded-nanocapsules film as a potential candidate for treating skin disorders: preparation, characterization, and antibacterial properties. *International Journal of Pharmaceutics* 633, 122608.
48. Santos, J.T., Marcucci, M.C., Santos, M.L.d., D'Alpino, P.H.P., 2023. Exploratory cross-sectional study of the use of a green propolis-based ointment in the treatment of skin tears in elderly hospitalized patients. *Res, Soc Dev* 12(4), e12412441061.
49. Sen, C.K., 2021. Human wound and its burden: updated 2020 compendium of estimates. *Adv Wound Care* 10(5), 281-292.
50. Song, Y.H., Zhu, Y.T., Ding, J., Zhou, F.Y., Xue, J.X., Jung, J.H., Li, Z.J., Gao, W.Y., 2016. Distribution of fibroblast growth factors and their roles in skin fibroblast cell migration. *Mol Med Rep* 14(4), 3336-3342.
51. Strecker-McGraw, M.K., Jones, T.R., Baer, D.G., 2007. Soft Tissue Wounds and Principles of Healing. *Emergency Medicine Clinics of North America* 25(1), 1-22.
52. Thomas, D.C., Tsu, C.L., Nain, R.A., Arsat, N., Fun, S.S., Sahid Nik Lah, N.A., 2021. The role of debridement in wound bed preparation in chronic wound: A narrative review. *Ann Med Surg* 71, 102876.
53. Tice, R.R., Agurell, E., Anderson, D., Burlinson, B., Hartmann, A., Kobayashi, H., Miyamae, Y., Rojas, E., Ryu, J.-C., Sasaki, Y.F., 2000. Single cell gel/comet assay: Guidelines for in vitro and in vivo genetic toxicology testing. *Environ Mol Mutagen* 35(3), 206-221.
54. Volkov, V.A., Voronkov, M.V., Misin, V.M., Fedorova, E.S., Rodin, I.A., Stavrianidi, A.N., 2021. Aqueous propylene glycol extracts from medicinal plants: chemical composition, antioxidant activity, standardization, and extraction kinetics. *Inorg Mater* 57(14), 1404-1412.

55. Wang, P.H., Huang, B.S., Horng, H.C., Yeh, C.C., Chen, Y.J., 2018. Wound healing. *J Chin Med Assoc* 81(2), 94-101.
56. Wilgus, T.A., 2008. Immune cells in the healing skin wound: Influential players at each stage of repair. *Pharmacol Res* 58(2), 112-116.
57. Yang, H., Song, L., Zou, Y., Sun, D., Wang, L., Yu, Z., Guo, J., 2021. Role of hyaluronic acids and potential as regenerative biomaterials in wound healing. *ACS Appl Bio Mater* 4(1), 311-324.
58. Yogiraj, V., Goyal, P., Chauhan, C.S., Goyal, A., Vyas, B., 2014. *Carica papaya* Linn: an overview. *Int J Herb Med* 2, 1-8.
59. Yuan, H., Ma, Q., Ye, L., Piao, G., 2016. The traditional medicine and modern medicine from natural products. *Molecules* 21(5), 559.

Disclaimer/Publisher's Note: The statements, opinions and data contained in all publications are solely those of the individual author(s) and contributor(s) and not of MDPI and/or the editor(s). MDPI and/or the editor(s) disclaim responsibility for any injury to people or property resulting from any ideas, methods, instructions or products referred to in the content.